Activin E-ACVR1C crosstalk controls energy storage via suppression of adipose lipolysis in mice

Rene C. Adam[a], Dwaine S. Pryce[a], Joseph S. Lee[a], Yuanqi Zhao[a], Ivory J. Mintah[a], Soo Min[a], Gabor Halasz[a], Jason Mastaitis[a], Gurinder S. Atwal[a], Senem Aykul[a], Vincent Idone[a], Aris N. Economides[a], Luca A. Lotta[a], Andrew J. Murphy[a], George D. Yancopoulos[a,b], Mark W. Sleeman[a], Viktoria Gusarova[a,b]

[a]Regeneron Pharmaceuticals, Tarrytown, New York, 10591, USA

[b]To whom correspondence may be addressed: Viktoria Gusarova, PhD

Regeneron Pharmaceuticals, Inc.

777 Old Saw Mill River Road, Tarrytown, New York, 10591, USA

Phone number: +1-914-847-3018

email: Viktoria.Gusarova@regeneron.com

[b]To whom correspondence may be addressed: George D. Yancopoulos, MD, PhD

Regeneron Pharmaceuticals, Inc.

777 Old Saw Mill River Road, Tarrytown, New York, 10591, USA

Phone number: +1-914-847-7423

email: George.Yancopoulos@regeneron.com

Author contributions: R.C.A., G.H., J.M., G.S.A., V.I., A.N.E. and V.G. designed research. R.C.A., D.S.P., J.S.L., Y.Z., I.J.M., S.M. and G.H. performed research and analyzed data. S.A. contributed new reagents/analytic tools. R.C.A., J.M., A.N.E., L.A.L., A.J.M., G.D.Y., M.W.S. and V.G. wrote the paper.

Competing interest statement: R.C.A., D.S.P., J.S.L., Y.Z., I.J.M., S.M., G.H., J.M., G.S.A., S.A., V.I., A.N.E., L.A.L., A.J.M., G.D.Y., M.W.S. and V.G. are employees and shareholders at Regeneron Pharmaceuticals.

Classification: BIOLOGICAL SCIENCES / Cell Biology

Keywords: INHBE (Activin E), ACVR1C; body fat distribution; lipolysis; diabetes

This PDF file includes:

Figures S1 to S5

Legends for Datasets S1 and S2

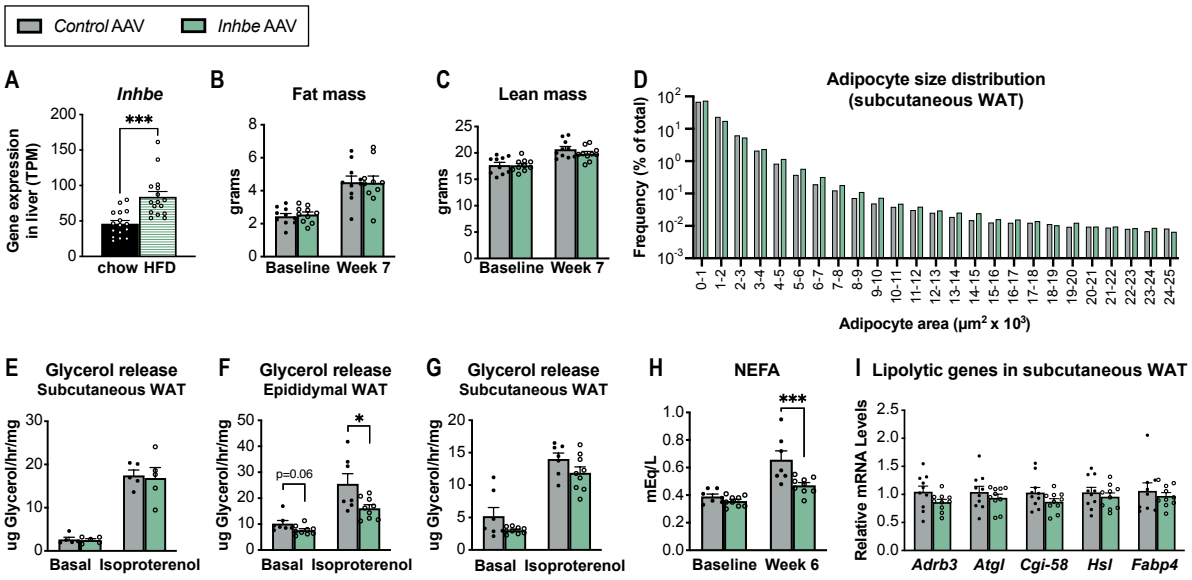

Fig. S1. Activin E is increased upon high fat feeding and impairs adipose lipolysis. (*A*) Hepatic *Inhbe* gene expression on chow and high fat diet (HFD) (TPM: transcripts per million) (n = 16). (*B* and *C*) Body composition of male *Control* AAV and *Inhbe* AAV-treated WT mice. Fat mass (*B*) and lean mass (*C*) were analyzed by echoMRI (n = 10). (*D*) Adipocyte morphology and size distribution measured by imaging software in H&E-stained subcutaneous WAT sections (n = 641490 cells for *Control* AAV and 585827 cells for *Inhbe* AAV analyzed from 10 mice/group). (*E*) *Ex vivo* lipolysis with subcutaneous WAT explants from WT mice under basal and isoproterenol-stimulated conditions (n = 5). (*F* and *G*) *Ex vivo* lipolysis with epididymal (*F*) and subcutaneous (*G*) WAT explants from *db/db* mice (n = 7 for *Control* AAV, 9 for *Inhbe* AAV). (*H*) Fasted plasma NEFA levels in *db/db* mice (n = 7 for *Control* AAV, 9 for *Inhbe* AAV). (*I*) Subcutaneous WAT mRNA levels of genes involved in adipose lipolysis, relative to *Control* AAV (n = 10). Mean ± s.e.m. are shown in all graphs besides (*D*), where mean is shown. *P<0.05, ***P<0.001 relative to *Control* AAV.

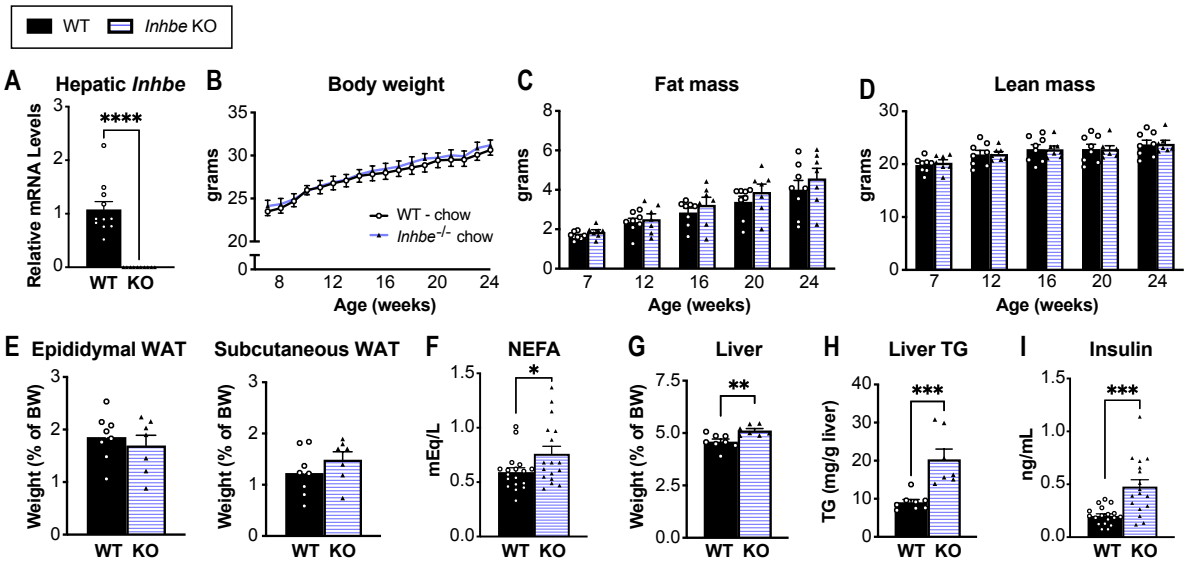

Fig. S2. *Inhbe* KO mice exhibit increased fasting liver lipid content on chow diet. (*A*) Hepatic Liver mRNA levels of *Inhbe* in WT and *Inhbe*$^{-/-}$ mice (n = 10-11). (*B*) Body weights in 7–24 week old male WT and *Inhbe*$^{-/-}$ mice on chow diet (n = 7-8). (*C* and *D*) Body composition measured by echoMRI to determine fat (*C*) and lean mass (*D*) of male WT and *Inhbe*$^{-/-}$ mice on chow diet (n = 7-8). (*E*) Weights of visceral (epididymal) and subcutaneous (inguinal) white adipose tissue on chow diet (n = 7-8). (*F*) Plasma NEFA levels on chow diet (n = 15-16). (*G* and *H*) Fasted liver weight (*G*) and hepatic triglyceride content (*H*) in *Inhbe*$^{-/-}$ mice on chow diet (n = 7-8). (*I*) Plasma insulin levels in *Inhbe*$^{-/-}$ mice on chow diet (n = 17-18). Mean ± s.e.m. are shown in all graphs. *P<0.05, **P<0.01, ***P<0.001.

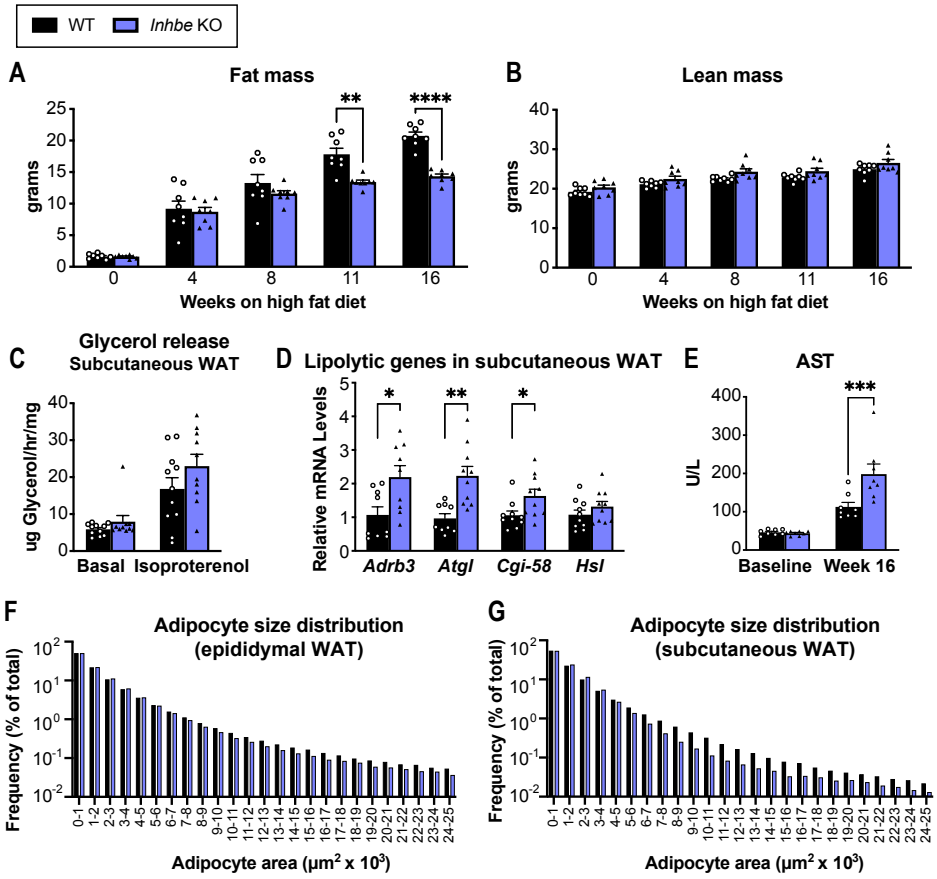

Fig. S3. *Inhbe* KO mice accrue less fat mass on HFD. (*A* and *B*) Body composition measured by echoMRI to determine fat (*A*) and lean mass (*B*) of male WT and *Inhbe*$^{-/-}$ mice on HFD (n = 8). (*C*) *Ex vivo* lipolysis with subcutaneous WAT explants from WT and *Inhbe*$^{-/-}$ mice on HFD (n = 10-11). (*D*) Subcutaneous WAT mRNA levels of genes involved in adipose lipolysis (n = 9-10). (*E*) Plasma AST levels in *Inhbe*$^{-/-}$ mice before and after 16 weeks of HFD (n = 8). (*F* and *G*) Adipocyte morphology and size distribution measured by imaging software in H&E-stained epididymal (*F*) and subcutaneous (*G*) WAT sections following HFD (n = 1288100 cells for WT epididymal WAT, 1034341 for *Inhbe*$^{-/-}$ epididymal WAT, 1395482 for WT subcutaneous WAT, and 1140473 cells for *Inhbe*$^{-/-}$ subcutaneous WAT analyzed from 10-11 mice/group). Mean ± s.e.m. are shown in all graphs besides (*F* and *G*), where mean is shown. *P<0.05, **P<0.01, ****P<0.0001.

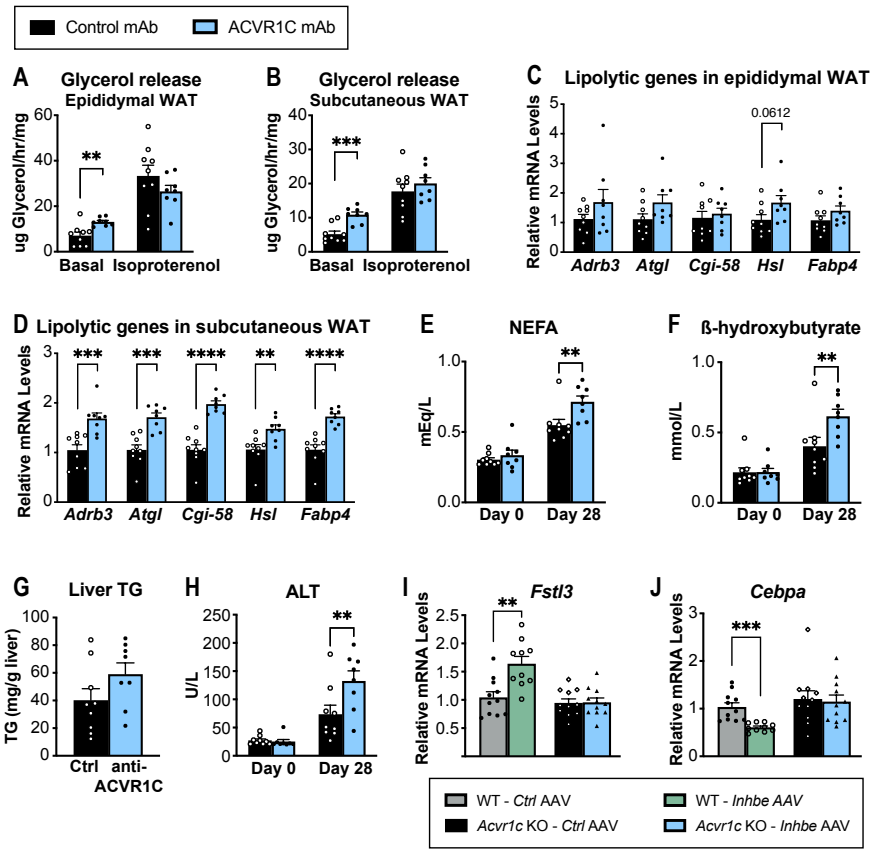

Fig. S4. ACVR1C inhibition parallels phenotypes in *Inhbe* KO mice. (*A* and *B*) *Ex vivo* lipolysis with epididymal (*A*) and subcutaneous (*B*) WAT explants from control mAb or ACVR1C mAb-treated mice (*n* = 8-9). (*C* and *D*) mRNA levels of genes involved in adipose lipolysis in epididymal (*C*) and subcutaneous (*D*) WAT (*n* = 8-9). (*E* and *F*) Fasted plasma NEFA (*E*) and beta-hydroxybutyrate (*F*) levels on HFD (*n* = 8-9). (*G* and *H*) Fasted hepatic triglyceride content (*G*), and plasma ALT levels (*H*) in Control mAb or ACVR1C mAb-treated mice (*n* = 8-9). (*I* and *J*) Epididymal WAT mRNA levels of activin target gene *Fstl3* (*I*) and adipose transcription factor *Cebpa* (*J*), relative to *Control* AAV in WT and *Acvr1c*$^{-/-}$ mice (*n* = 10-11). Mean ± s.e.m. are shown in all graphs. **P<0.01, ***P<0.001, ****P<0.0001.

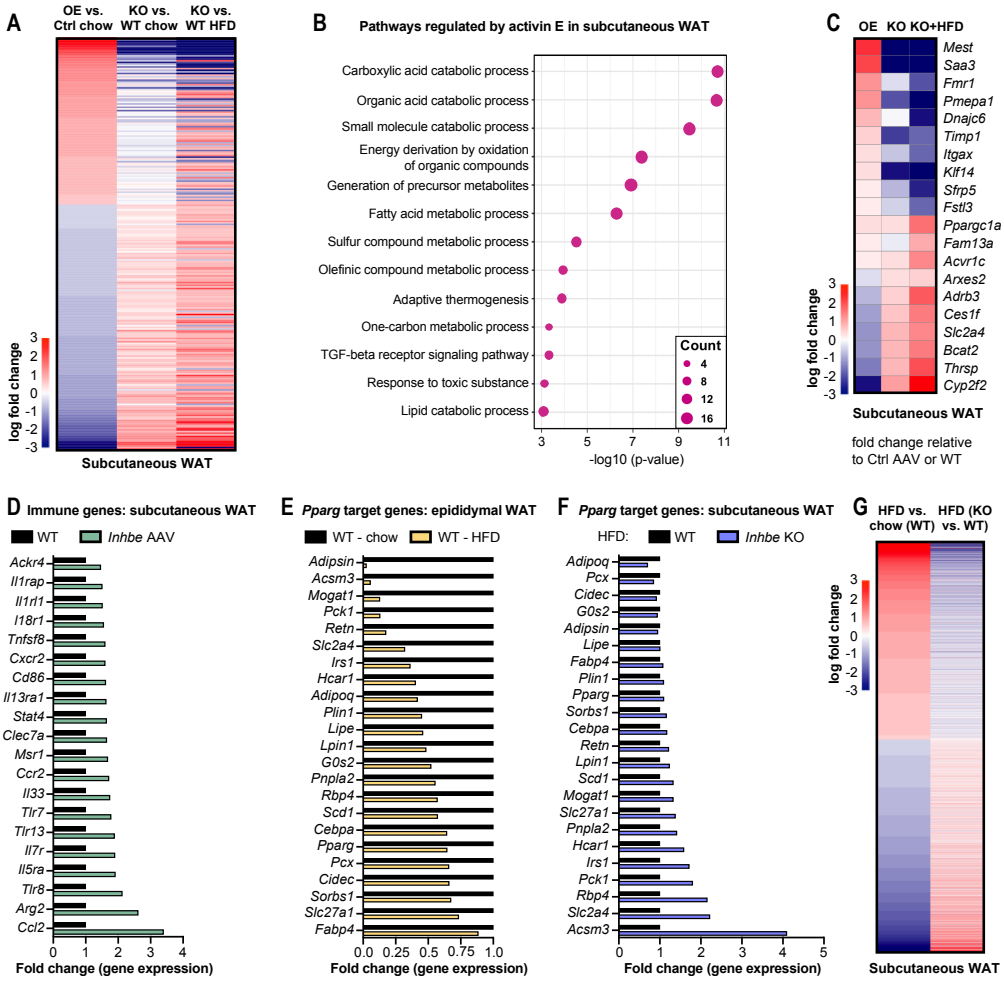

Fig. S5. Activin E control adipose metabolic gene expression. (*A*) Heatmap of subcutaneous adipose transcriptome signatures comparing *Inhbe* over-expression, *Inhbe* KO on chow and high fat diet (HFD) vs. control-treated or WT mice, respectively. (*B*) Dot plots showing top biological pathways for oppositely regulated genes (*Inhbe* over-expression vs. KO) in subcutaneous WAT. (*C*) Heatmap showing examples of oppositely regulated genes (*Inhbe* over-expression vs. KO) in subcutaneous WAT. (*D*) Relative gene expression levels of immune-related genes in subcutaneous WAT, comparing *Inhbe* over-expression vs. control. (*E*) Relative gene expression levels of PPARG target genes in epididymal WAT, comparing WT mice on chow vs. high fat diet. (*F*) Relative gene expression levels of PPARG target genes in subcutaneous WAT, comparing *Inhbe* KO and WT mice on high fat diet. (*G*) Heatmap of subcutaneous adipose

transcriptome signatures comparing WT chow vs. HFD, and *Inhbe* KO vs. WT on high fat diet (HFD), demonstrating *Inhbe* LOF reverses many of the HFD effects seen in WT mice.

Dataset S1: List of oppositely regulated genes by *Inhbe* over-expression and knockout in epididymal and subcutaneous adipose tissue

Dataset S2: Pathway analysis of differentially expressed genes in epididymal and subcutaneous adipose tissue upon *Inhbe* over-expression and knockout.